

THREE DIMENSIONAL SIMULATION OF LARGE-ASPECT-RATIO ELLIPSE-SHAPED CHARGED-PARTICLE BEAM PROPAGATION*

R. Bhatt, J. Zhou, and C. Chen

Plasma Science and Fusion Center, MIT, Cambridge, MA 02139

Abstract

A new equilibrium theory for a large-aspect-ratio ellipse-shaped charged-particle beam in a non-axisymmetric periodic permanent magnet focusing field has been developed recently [1]. A periodic beam equilibrium solution is obtained numerically from a set of generalized envelope equations. It is shown that the beam edges are well confined in both transverse directions, and that the equilibrium beam exhibits a periodic small-amplitude twist as it propagates. A two-dimensional particle-in-cell (PIC) code, PFB2D and a three-dimensional trajectory code, OMNITRAK [2] are used to verify the theoretical predictions in the paraxial limit. The influence of the beam image charge due to a conducting wall is assessed via both sets of simulations.

INTRODUCTION

High-intensity ribbon (thin sheet) beams are of great interest in the design and operation of particle accelerators, such as storage rings and rf and induction linacs, as well as vacuum electron devices, such as klystrons and traveling-wave tubes with periodic permanent magnet (PPM) focusing [1, 3 and refs therein], because of several remarkable properties. First, they can transport large amounts of beam currents with reduced intrinsic space-charge forces and energies. Second, they couple efficiently to rectangular rf structures. This combination of the space charge reduction and efficient coupling allows efficient rf generation in vacuum electronic devices, and efficient acceleration in particle accelerators. Third, elliptic beams provide an additional adjustable parameter (i.e., the aspect ratio) which may be useful for better matching a beam into a periodic focusing channel.

An equilibrium theory has been developed [1] for an elliptic cross-section space-charge-dominated beam in a non-axisymmetric periodic magnetic focusing field. A paraxial cold-fluid model is employed to derive generalized envelope equations which determine the equilibrium flow properties of ellipse-shaped beams with negligibly small emittance. A matched envelope solution is obtained numerically from the generalized envelope equations, and the results show that the beam edges in both transverse directions are well confined, and that the angle of the beam ellipse exhibits a periodic small-amplitude twist. Two-dimensional (2D) particle-in-cell (PIC) simulations with the Periodic Focused Beam 2D

(PFB2D) code show good agreement with the predictions of equilibrium theory as well as beam stability.

Both the equilibrium theory and the PFB2D simulations predict a periodic twist of the orientation of the semi-major and semi-minor axes of the elliptic beam as it propagates longitudinally. Because of this, the beam boundary can no longer strictly be considered that of an elliptic cylinder, but takes a more complicated, axially twisting form. At each longitudinal position, however, the equilibrium theory and the PFB2D code both assume a longitudinally invariant beam (oriented at the local value of the twist angle) for the purposes of electric field calculations. While it can be argued that the field corrections introduced by a proper treatment of the twisted structure will be negligible for small twist angles, a quantitative assessment of these effects is lacking.

The three-dimensional trajectory code, OMNITRAK, is capable of resolving the 3D structure of the beam while self-consistently calculating the resultant space-charge electric fields. We employ it here for three purposes: firstly, to assess the impact of the varying twist angle on beam dynamics through corrections to the self-fields, secondly, as an independent verification of the envelope solution, and thirdly, as a benchmark for the PFB2D simulation code.

EQUILIBRIUM THEORY

We consider a high-intensity, space-charge-dominated beam, in which kinetic (emittance) effects are negligibly small. The beam can be adequately described by cold-fluid equations. In the paraxial approximation, the steady-state cold-fluid equations for time-stationary flow ($\partial/\partial t = 0$) in cgs units are [1, 4]

$$\beta_b c \partial n_b / \partial s + \nabla_{\perp} \cdot (n_b \mathbf{V}_{\perp}) = 0, \quad (1)$$

$$\nabla_{\perp}^2 \phi^s = \beta_b^{-1} \nabla_{\perp}^2 A_z^s = -4\pi q n_b, \quad (2)$$

$$n_b \left(\beta_b c \frac{\partial}{\partial s} + \mathbf{V}_{\perp} \cdot \nabla_{\perp} \right) \mathbf{V}_{\perp} = \frac{q n_b}{\gamma_b m} \left[-\frac{1}{\gamma_b^2} \nabla_{\perp} \phi^s + \beta_b \hat{\mathbf{e}}_z \times \mathbf{B}_{\perp}^{ext} + \frac{\mathbf{V}_{\perp}}{c} \times B_z^{ext}(s) \hat{\mathbf{e}}_z \right], \quad (3)$$

where $s = z$, $\mathbf{x}_{\perp} = x\hat{\mathbf{e}}_x + y\hat{\mathbf{e}}_y$, $\nabla_{\perp} = \partial/\partial \mathbf{x}_{\perp}$, q and m are the particle charge and rest mass, respectively, n_b is the particle density, \mathbf{V}_{\perp} is the transverse flow velocity, $\gamma_b = (1 - \beta_b^2)^{-1/2}$ is the relativistic mass factor, use has been made of $\beta_z = V_z/c \equiv \beta_b = const$, c is the speed of light in vacuum, and the self-electric field

*Work supported by the U.S. DoE, office of HEP, DE-FG02-95ER40919, Office of FES, DE-FG02-01ER54662, Air Force Office of Scientific Research, F49620-03-1-0230, and the MIT Deshpande Center for Technological Innovation.

\mathbf{E}^s and self-magnetic field \mathbf{B}^s are determined from the scalar potential ϕ^s and vector potential $A_z^s \hat{\mathbf{e}}_z$, i.e., $\mathbf{E}^s = -\nabla_{\perp} \phi^s$ and $\mathbf{B}^s = \nabla_{\perp} \times A_z^s \hat{\mathbf{e}}_z$. We seek solutions to Eqs. (1)-(3) of the form [4]

$$n_b(\mathbf{x}_{\perp}, s) = \frac{N_b}{\pi a(s)b(s)} \Theta \left[1 - \frac{\tilde{x}^2}{a^2(s)} - \frac{\tilde{y}^2}{b^2(s)} \right], \quad (5)$$

$$\mathbf{V}_{\perp}(\mathbf{x}_{\perp}, s) = [\mu_x(s)\tilde{x} - \alpha_x(s)\tilde{y}] \beta_b c \hat{\mathbf{e}}_{\tilde{x}} + [\mu_y(s)\tilde{y} + \alpha_y(s)\tilde{x}] \beta_b c \hat{\mathbf{e}}_{\tilde{y}}. \quad (6)$$

In Eqs. (5) and (6), $\mathbf{x}_{\perp} = \tilde{x} \hat{\mathbf{e}}_{\tilde{x}} + \tilde{y} \hat{\mathbf{e}}_{\tilde{y}}$ is a transverse displacement in the twisted coordinate system illustrated in Fig. 1; $\theta(s)$ is the twist angle of the ellipse; $\Theta(x) = 1$ if $x > 0$ and $\Theta(x) = 0$ if $x < 0$; and the functions $a(s)$, $b(s)$, $\mu_x(s)$, $\mu_y(s)$, $\alpha_x(s)$, $\alpha_y(s)$ and $\theta(s)$ are to be determined self-consistently [1].

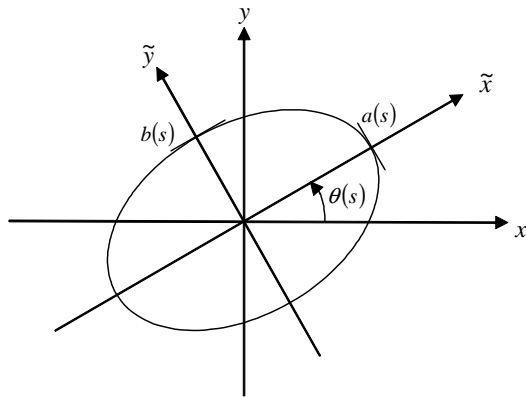


Figure 1: Laboratory and twisted coordinate systems showing the elliptical beam envelopes $a(s)$ and $b(s)$ and the twist angle $\theta(s)$.

Using the expressions above and following the technique in [1, 4], it can be shown that both the equilibrium continuity equation (1) and force equation (3) can be reduced to a set of generalized beam envelope equations [4] in the dynamical variables $a(s)$, $b(s)$, $\mu_x(s) \equiv a^{-1} da/ds$, $\mu_y(s) \equiv b^{-1} db/ds$, $\alpha_x(s)$, $\alpha_y(s)$ and $\theta(s)$. These envelope equations can be integrated directly, subject to periodic boundary conditions, and a Newton's method search applied in order to find matched solutions of the sort shown in Figure 2 for a 6:1 aspect ratio beam of semi-major axis $a = 3.73$ mm and $b = 0.62$ mm. This beam corresponds to the nonrelativistic example of Ref [1] at a voltage of 2.29 kV and with a current of 0.11 A focused by a 1.9 cm period non-axisymmetric periodic magnetic field in a paraxial representation.

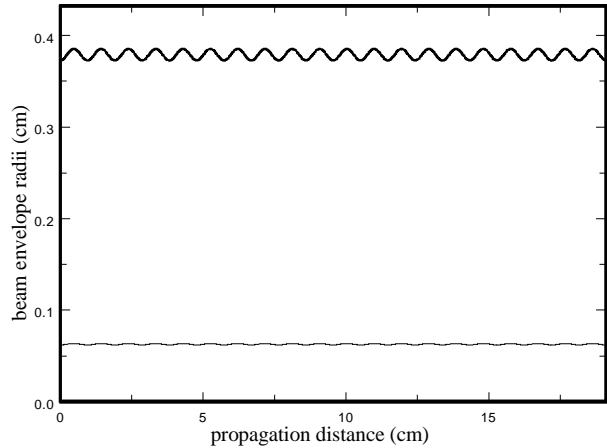


Figure 2: The envelope equations are directly integrated to obtain plots of the elliptical envelope semi-major radius $a(s)$ (thick line), and semi-minor radius $b(s)$ (thin line) are shown as a function of the propagation distance s .

SIMULATION

The envelope equations do not incorporate the effects of image charge, however, they are included in the PFB2D particle-in-cell code and in the 3D OMNITRAK code. In Figure 3, the dashed lines show the envelopes as computed by a PFB2D calculation incorporating image-charge effects from the conducting wall boundaries of a 12 mm x 12 mm beam tunnel. We note that the presence of the beam tunnel does not severely affect the beam. Additional scalloping is seen as compared to the envelope solution of Figure 2, but this is at a manageable level.

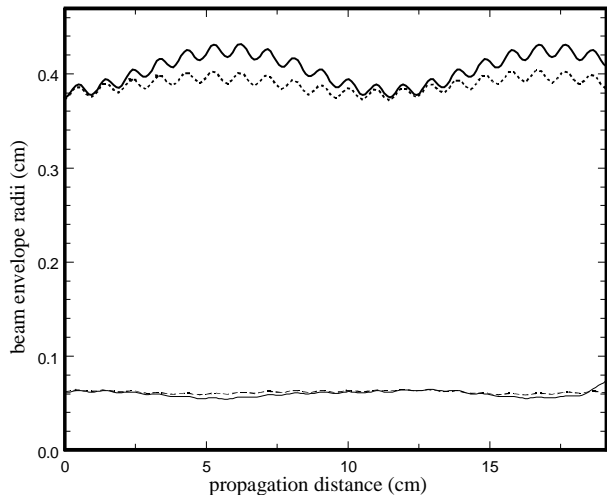


Figure 3: The rms envelopes are computed in a 12 mm x 12 mm rectangular beam tunnel using the PFB2D code (dashed lines) and the 3D OMNITRAK code (solid lines) with paraxial magnetic fields. The elliptical envelope semi-major radius $a(s)$ (thick lines), and semi-minor radius $b(s)$ (thin lines) are shown as a function of the propagation distance s .

The solid lines in Figure 3 indicate the envelopes as computed using the OMNITRAK code. We notice further

beam scalloping when compared with the PFB2D code results, however it is not clear whether this effect is due to the incorporation of 3D effects or merely a result of additional numerical errors, since the 3D code, by necessity, must use a coarser mesh than the 2D code. Nonetheless, the simulations do place an upper bound on the deleterious effect of the 3D effects. Beam scalloping is seen, but there is no discernable beam loss.

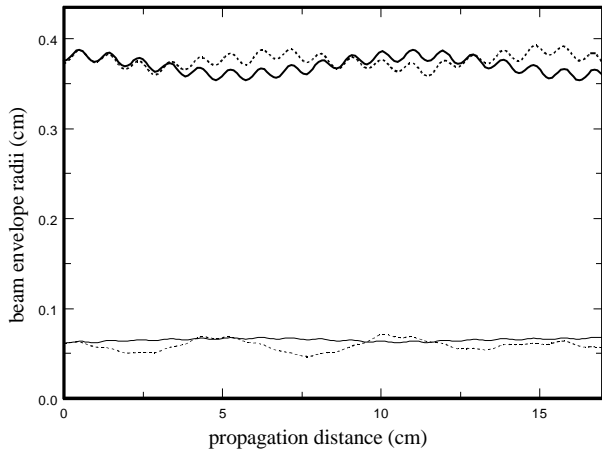


Figure 4: The rms envelopes are computed in a 10.7 mm x 7 mm rectangular beam tunnel using the PFB2D code with a paraxial magnetic field (dashed lines) and the 3D OMNITRAK code with a realistic field map from Ref [5] (solid lines). The elliptical envelope semi-major radius $a(s)$ (thick lines), and semi-minor radius $b(s)$ (thin lines) are as a function of the propagation distance s .

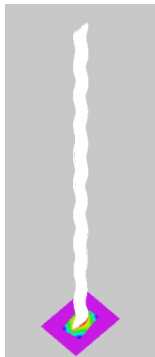


Figure 5: The fluid trajectories for the realistic field map case are computed using the 3D OMNITRAK code and shown over a 10 period focusing lattice. The twisted structure of the beam is evident.

When we reduce the beam tunnel size to 10.7 mm x 7 mm, we expect the image-charge effects to increase. The results of this modification are shown in Figure 4 where the dashed lines indicate the PFB2D results. Note that the greatest change (as compared to the larger tunnel of

Figure 3) is the additional scalloping seen in the beam minor radius. Nonetheless, confinement is maintained.

The solid lines in Figure 4 indicate the OMNITRAK results for the smaller beam tunnel. Unlike all the previous results, however, the beam in this simulation is not focused using a paraxial representation of the magnetic field, but rather by a realistic imported magnetic field map computed using the OPERA3D model of Ref. [5]. Thus we see that this elliptic beam can be focused using the non-axisymmetric ppm scheme with a physically achievable magnetic field while self-consistently incorporating 3D space-charge effects. Figure 5 shows the fluid trajectories in this simulation where the twisted beam structure is evident.

CONCLUSION

The validity of the non-axisymmetric periodic permanent magnet focusing theory of Ref [1] is established through 2D simulations using the PFB2D code as well as 3D simulation using the commercial trajectory code OMNITRAK. The beam is found to be well-confined in all cases considered, and its qualitative behavior is as predicted by the theory. The average envelope radii are also close to theoretical predictions, however larger envelope oscillations are seen with the 3D simulations than the 2D simulations. Future higher resolution 3D studies may establish that this is an artifact of finite resolution in the electric field calculations. Significant image charge effects are not seen in the cases considered.

REFERENCES

- [1] J. Zhou, R. Bhatt and C. Chen, submitted to Phys. Rev. Lett (2005).
- [2] OMNITRAK software, copyright Field Precision, Albuquerque, NM.
- [3] R. Bhatt and C. Chen, Phys. Rev. ST Accel. Beams 8, 104201 (2005).
- [4] R. Pakter and C. Chen, Phys. Rev. E 62, 2789 (2000).
- [5] R. Bhatt, C. Chen, A. Radovinsky, and J. Zhou, "Three-Dimensional Design of a Non-Axisymmetric Periodic Permanent Magnetic Focusing System", PAC 2005.